A rapidly-adaptable intranasal replicon vaccine establishes mucosal immunity and protects against H5N1 and H7N9 influenza

SUPPLEMENTARY FIGURES

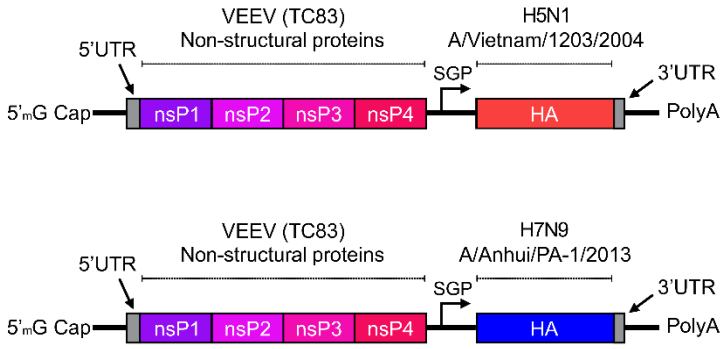

Supplementary Figure 1. Construct designs for the H5 and H7 replicon vaccine constructs. SGP = sub-genomic promoter.

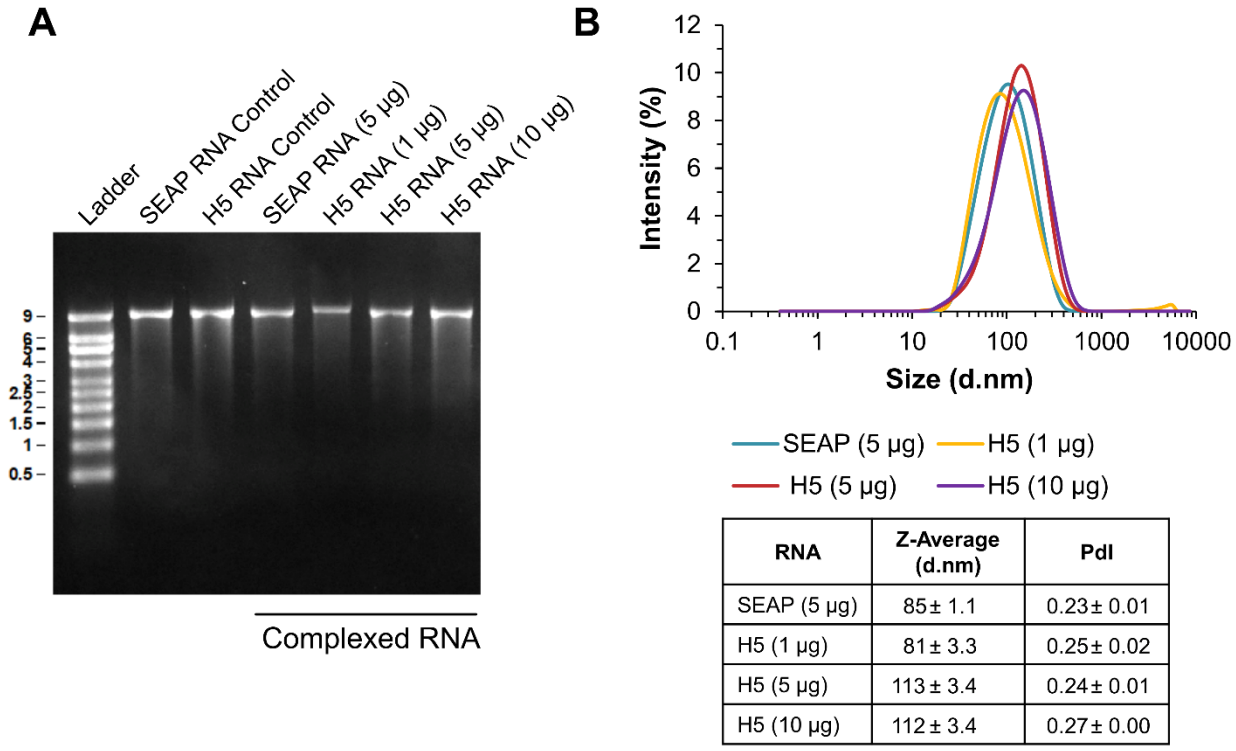

RNA	Z-Average (d.nm)	PdI
SEAP (5 µg)	85± 1.1	0.23± 0.01
H5 (1 µg)	81± 3.3	0.25± 0.02
H5 (5 µg)	113 ± 3.4	0.24± 0.01
H5 (10 µg)	112 ± 3.4	0.27± 0.00

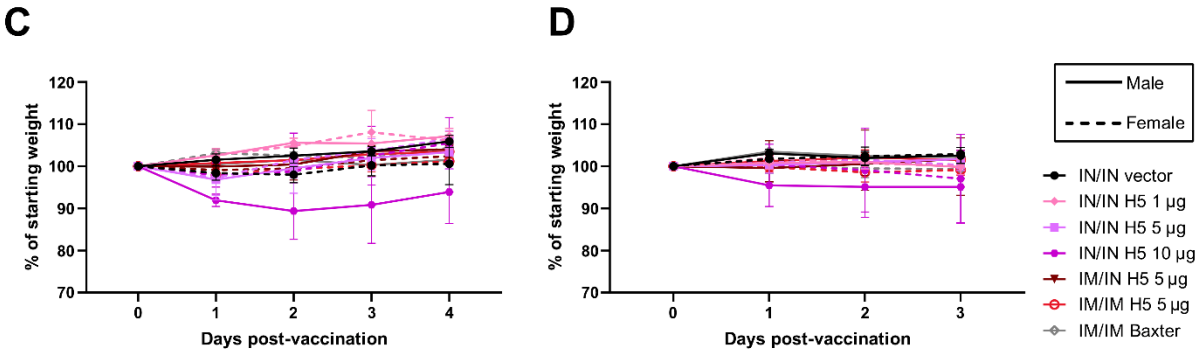

Supplementary Figure 2. Biophysical characterization and additional immune readouts for monovalent H5 replicon-NLC vaccine. (**A**) RNA size and integrity before complexing ("Control") and after extraction from the replicon-NLC complexes as measured by agarose gel electrophoresis (repeated twice with similar results). (**B**) Average size and polydispersity index (PdI) for replicon-NLC vaccine complexes, after measurement in triplicate. Particle size intensity distribution of replicon-NLC vaccine complexes as measured by dynamic light scattering. (**C-D**) Mouse body weights (C) post-prime and (D) post-boost. *n* = 6 (3M:3F) for vector control (SEAP) group and *n* = 8 (4M:4F) for experimental groups. Data are presented as (C, D) mean +/- SD. NLC = nanostructured lipid carrier; SEAP = secreted embryonic alkaline phosphatase; IN = Intranasal; IM = Intramuscular. Source data are provided as a Source Data file.

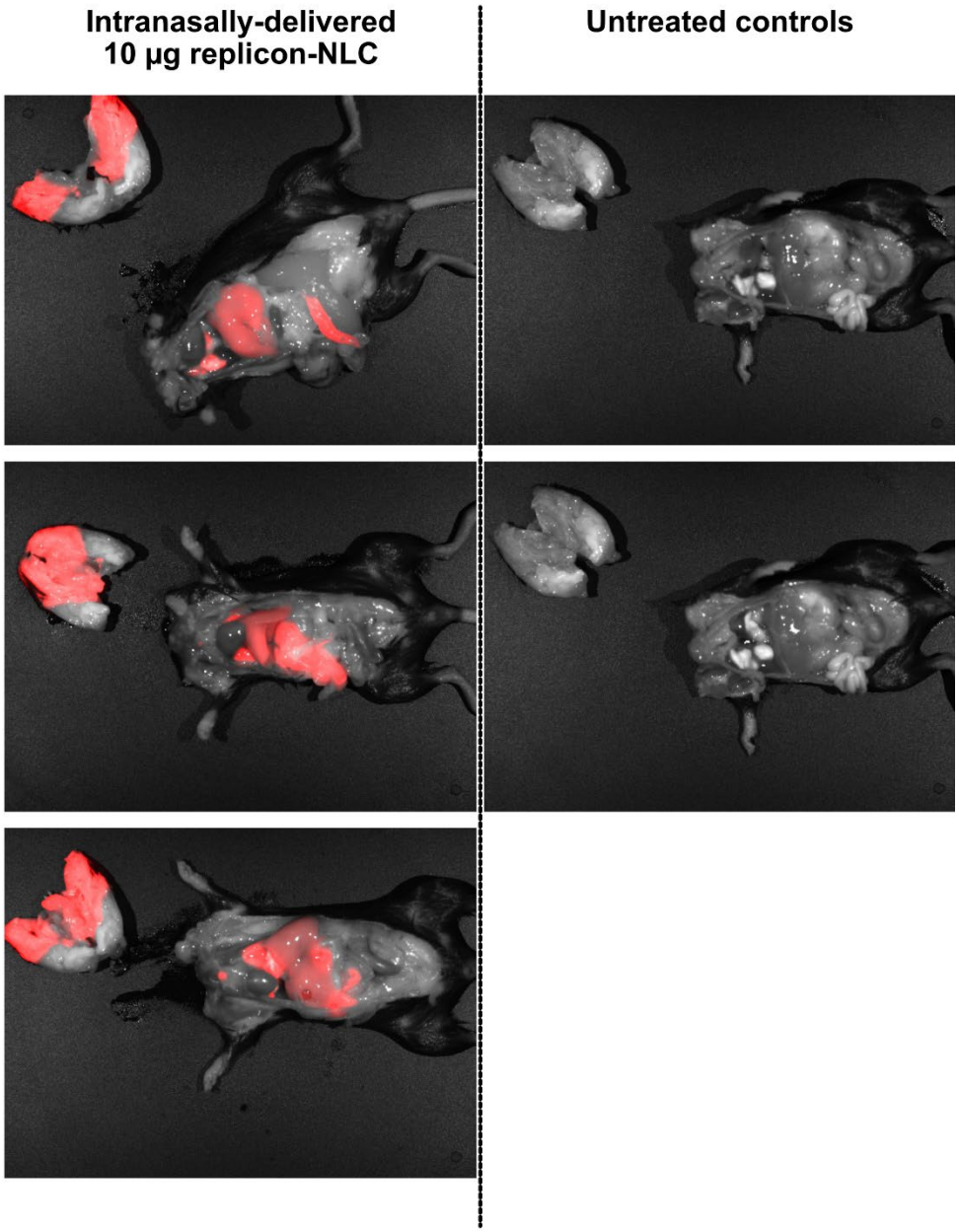

Supplementary Figure 3. Biodistribution of intranasally-delivered replicon-NLC vaccine. Prior to complexation, NLC particles were fluorescently stained by addition of Cy5.5 dye to a final dye concentration of 91 µg/mL. These fluourescently labeled NLCs were used in the downstream complexation reaction, yielding fluoresecnt replicon complexes.Ten µg of stained replicon-NLC in 50 µL total volume was then intranasally delivered to C57BL/6 mice under isoflurane sedation, identically to intranasally vaccinated mice. Four hours post administration, mice were euthanized and necropsied to allow visualization of stained NLC delivery by decapitation, bisection of heads to reveal the upper respiratory tissue (upper left of each image), and removal of sternums and ribcages to reveal the pleural cavity. Mice were then imaged using an Odyssey Pearl mouse imager using white light and 700 nm fluorescent imaging channels. NLC = nanostructured lipid carrier.

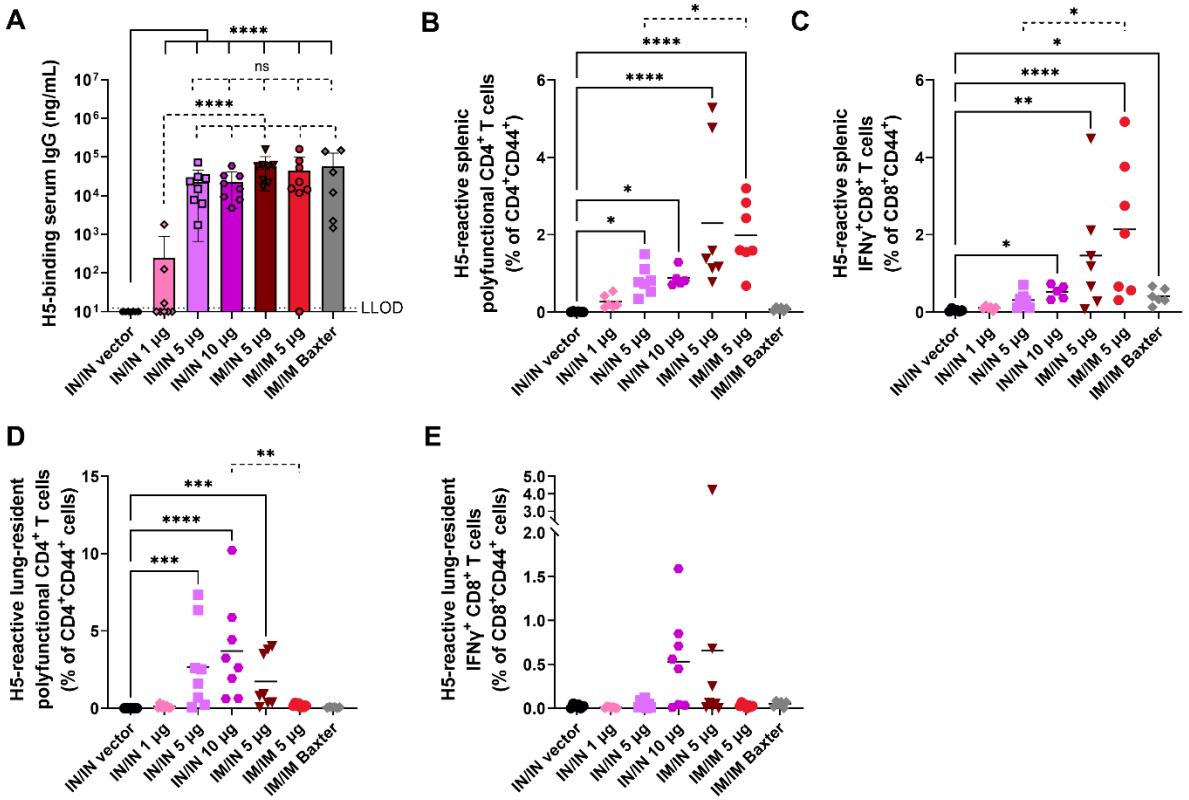

Supplementary Figure 4. Additional data from H5 replicon-NLC vaccine monovalent dosing study relevant to Figure 1. (**A**) Post-prime serum H5-binding IgG titers. Post-boost H5-reactive (**B**) splenic polyfunctional (IFN γ^+ IL-2$^+$ TNF α^+) CD4$^+$ T cells, (**C**) splenic IFN γ^+ CD8$^+$ T cells, (**D**) lung-resident (CD69$^+$) polyfunctional (IFN γ^+ IL-2$^+$ TNF α^+) CD4$^+$ T cells, and (**E**) lung-resident (CD69$^+$ CD103$^+$) IFN γ^+ CD8$^+$ T cells. (B-E) For all assays, $n = 6$ for vector control group and $n = 8$ for experimental groups. All groups were sex balanced. Two statistical hypotheses were tested within each figure, with filled lines showing comparisons to the vector control and dotted lines representing tests between key experimental groups. (A) Statistical analyses performed on log-transformed data using one-way ANOVA with Dunnett's (filled lines) or Tukey's (dotted lines) multiple comparisons test. (B-E) Statistical analysis represents Kruskal-Wallis test with Dunn's multiple comparisons (filled lines and dotted lines). Data are presented as (A) geometric mean +/- geometric SD. NLC = nanostructured lipid carrier; IN = Intranasal; IM = Intramuscular; LLOD = lower limit of detection; ns = not significant. * $p < 0.05$, ** $p < 0.01$, *** $p < 0.001$, **** $p < 0.0001$. Source data are provided as a Source Data file.

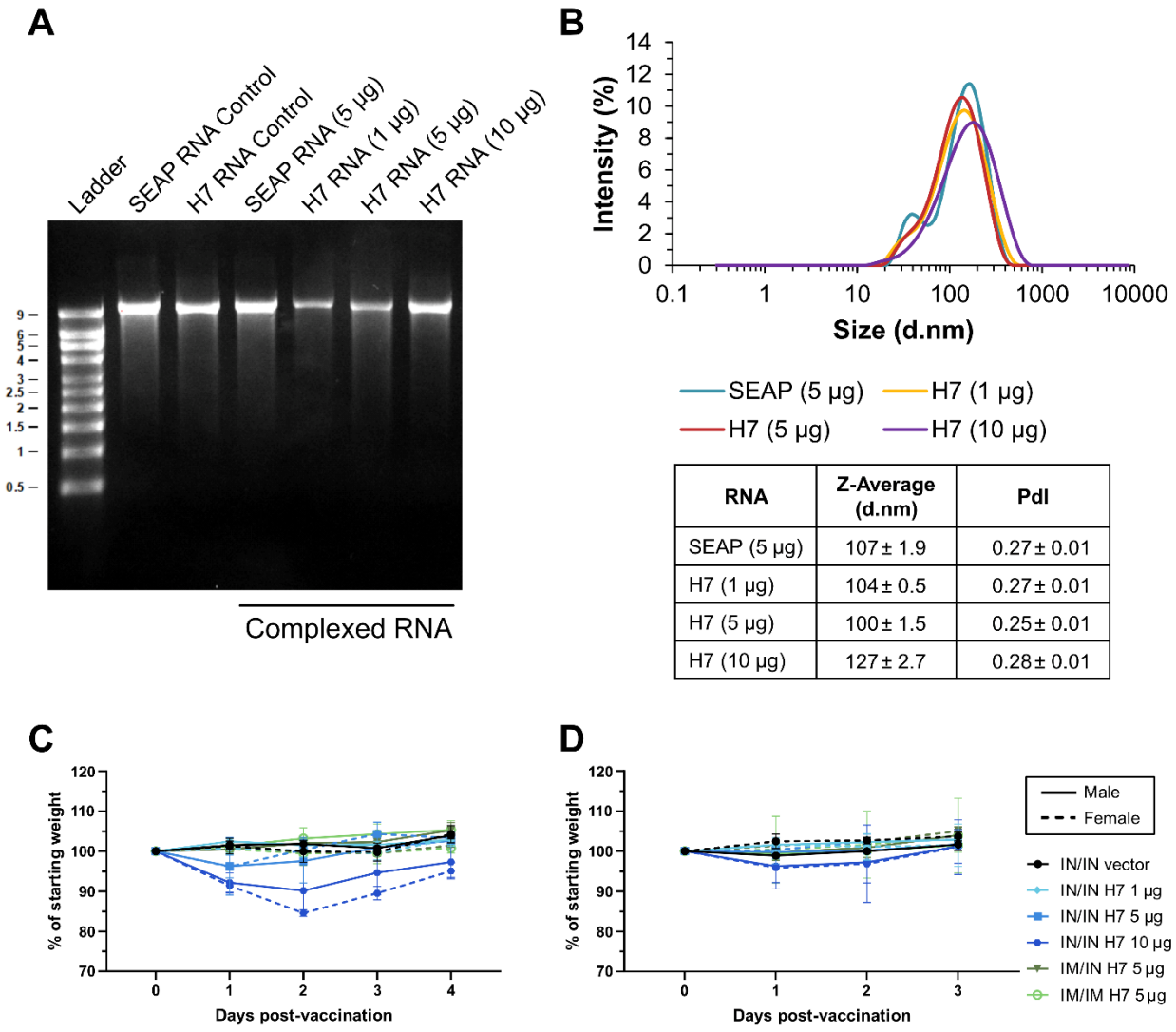

RNA	Z-Average (d.nm)	PdI
SEAP (5 µg)	107 ± 1.9	0.27 ± 0.01
H7 (1 µg)	104 ± 0.5	0.27 ± 0.01
H7 (5 µg)	100 ± 1.5	0.25 ± 0.01
H7 (10 µg)	127 ± 2.7	0.28 ± 0.01

Supplementary Figure 5. Biophysical characterization and additional immune readouts for monovalent H7 replicon-NLC vaccine. (**A**) RNA size and integrity before complexing ("Control") and after extraction from the replicon-NLC complexes as measured by agarose gel electrophoresis (repeated twice with similar results). (**B**) Average size and polydispersity index (PdI) for replicon-NLC vaccine complexes, after measurement in triplicate. Particle size intensity distribution of replicon-NLC vaccine complexes as measured by dynamic light scattering. (**C-D**) Mouse body weights (C) post-prime and (D) post-boost. *n* = 6 (3M:3F) for vector control (SEAP) group and *n* = 8 (4M:4F) for experimental groups. Data are presented as (C, D) mean +/- SD. NLC = nanostructured lipid carrier; SEAP = secreted embryonic alkaline phosphatase; IN = Intranasal; IM = Intramuscular. Source data are provided as a Source Data file.

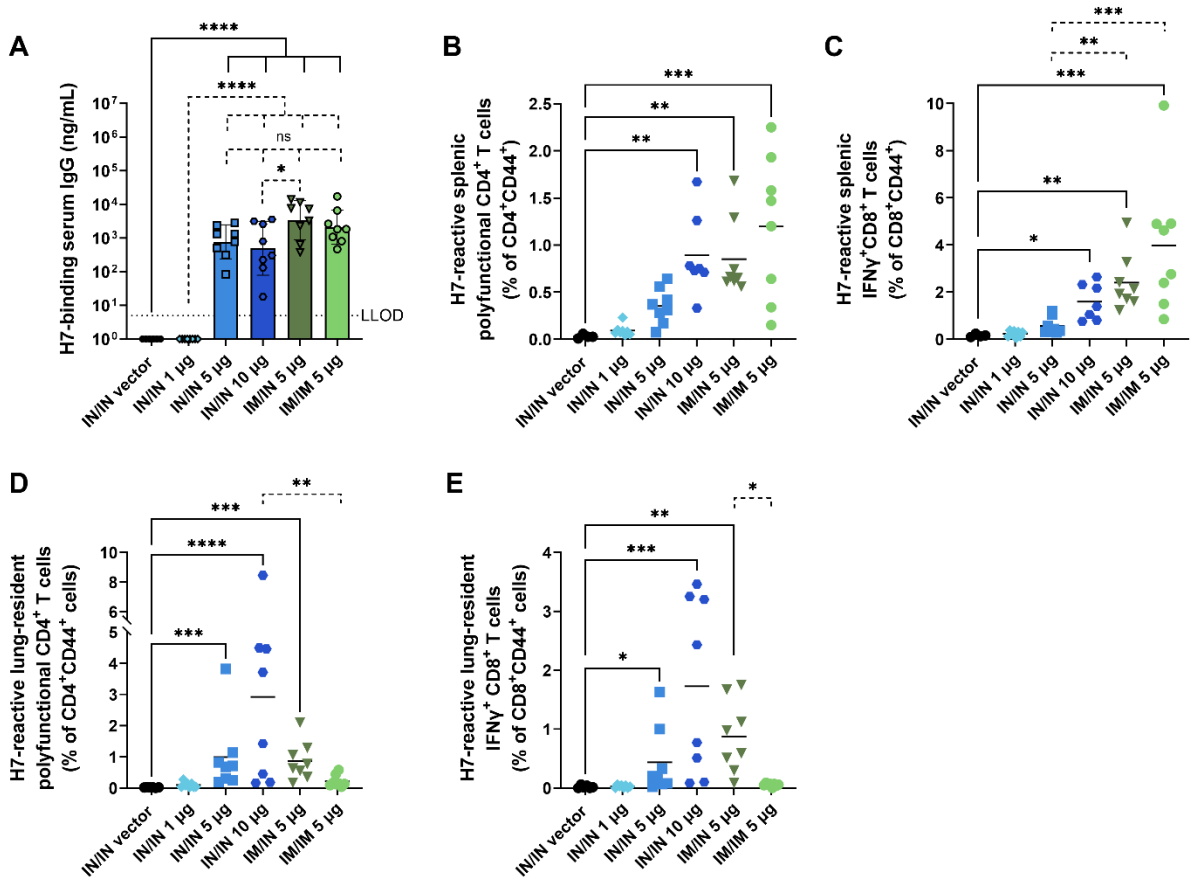

Supplementary Figure 6. Additional data from H7 replicon-NLC vaccine monovalent dosing study relevant to Figure 2. (**A**) Post-prime serum H7-binding IgG titers. Post-boost H7-reactive (**B**) splenic polyfunctional (IFN γ^+ IL-2$^+$ TNF α^+) CD4$^+$ T cells, (**C**) splenic IFN γ^+ CD8$^+$ T cells, (**D**) lung-resident (CD69$^+$) polyfunctional (IFN γ^+ IL-2$^+$ TNF α^+) CD4$^+$ T cells, and (**E**) lung-resident (CD69$^+$ CD103$^+$) IFN γ^+ CD8$^+$ T cells. For all assays, $n = 6$ for vector control group, $n = 8$ for experimental groups. All groups were sex balanced. Two statistical hypotheses were tested within each figure, with filled lines showing comparisons to the vector control and dotted lines representing tests between key experimental groups. (A) Statistical analyses performed on log-transformed data using one-way ANOVA with Dunnett's (filled lines) or Tukey's (dotted lines) multiple comparisons test. (B-E) Statistical analysis represents Kruskal-Wallis test with Dunn's multiple comparisons (filled lines [B-E] and dotted lines [C, D]) or Brown-Forsythe and Welch ANOVA with Dunnett's T3 multiple comparisons (dotted lines [B, E]). Data are presented as (A) geometric mean +/- geometric SD. NLC = nanostructured lipid carrier; IN = Intranasal; IM = Intramuscular; LLOD = lower limit of detection; ns = not significant. * $p < 0.05$, ** $p < 0.01$, *** $p < 0.001$, **** $p < 0.0001$. Source data are provided as a Source Data file.

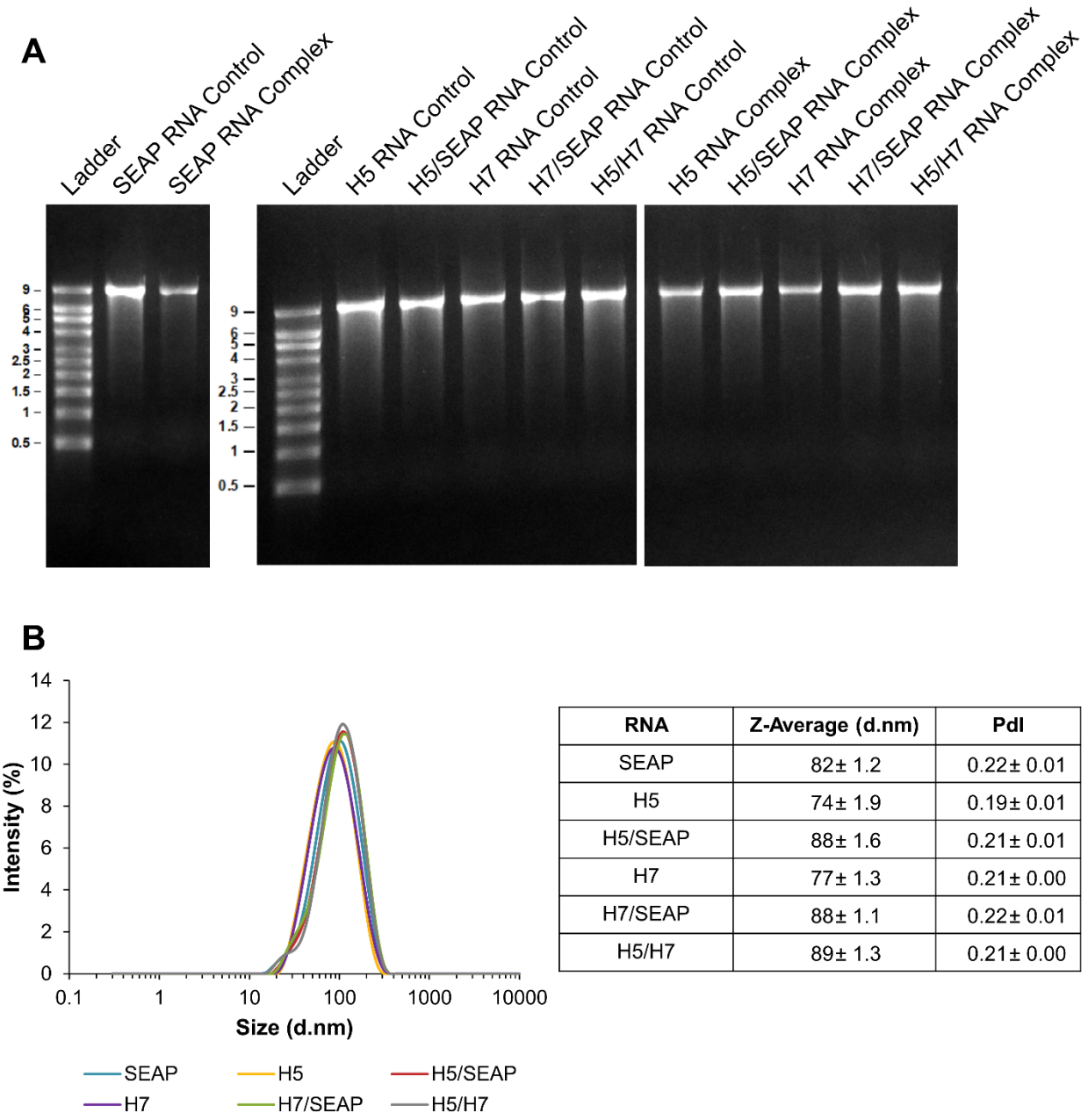

RNA	Z-Average (d.nm)	PdI
SEAP	82± 1.2	0.22± 0.01
H5	74± 1.9	0.19± 0.01
H5/SEAP	88± 1.6	0.21± 0.01
H7	77± 1.3	0.21± 0.00
H7/SEAP	88± 1.1	0.22± 0.01
H5/H7	89± 1.3	0.21± 0.00

Supplementary Figure 7. Biophysical characterization and additional immune readouts for bivalent H5/H7 replicon-NLC vaccine. (**A**) RNA size and integrity before complexing ("Control") and after extraction from the replicon-NLC complex ("Complex") as measured by agarose gel electrophoresis (repeated twice with similar results). (**B**) Average size and polydispersity index (PdI) for replicon-NLC vaccine complexes, after measurement in triplicate. Particle size intensity distribution of replicon-NLC vaccine complexes as measured by dynamic light scattering. Bivalent vaccines (H5/SEAP, H7/SEAP, and H5/H7) each represent 10 µg replicon total (5 µg of each replicon-NLC vaccine combined by simple mixing). NLC = nanostructured lipid carrier; SEAP = secreted embryonic alkaline phosphatase; IN = Intranasal; IM = Intramuscular. Source data are provided as a Source Data file.

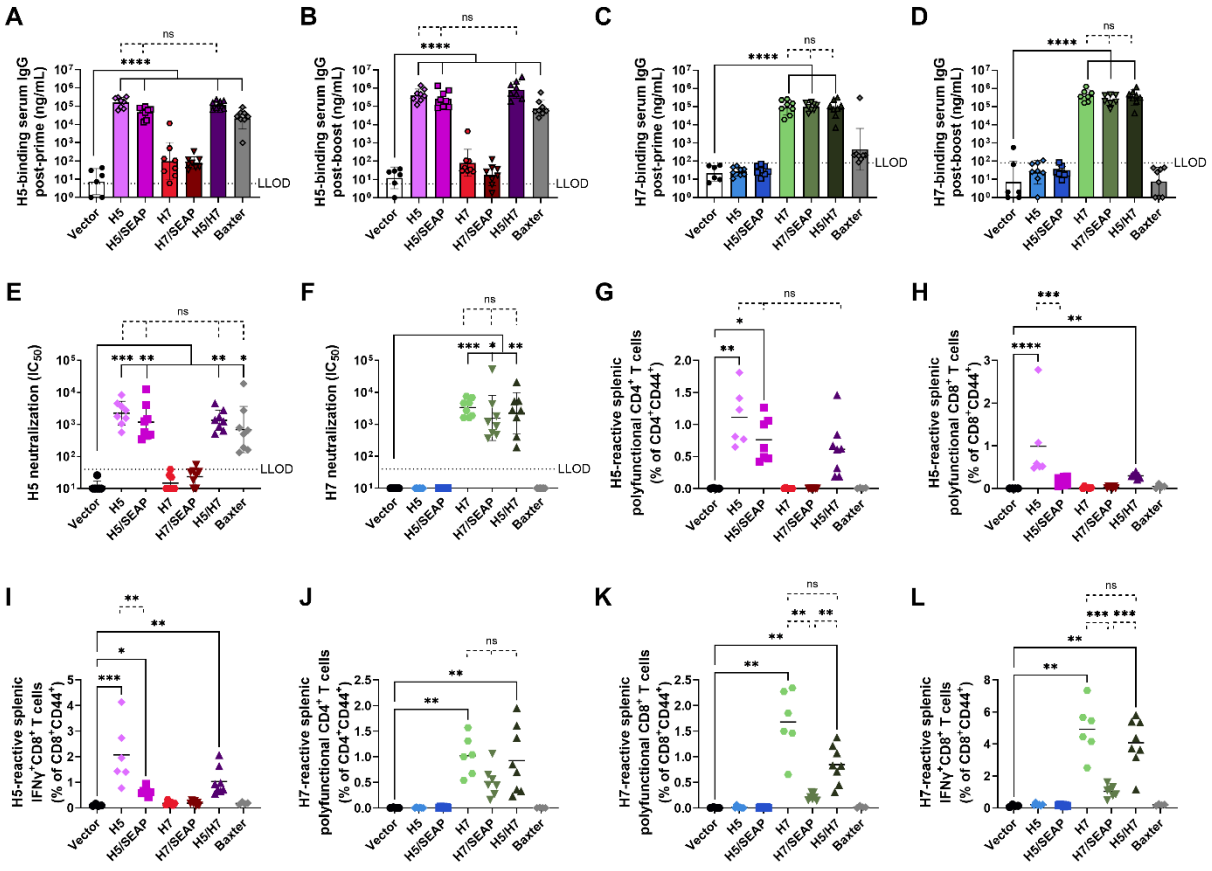

Supplementary Figure 8. Full bivalent intramuscular study systemic immunogenicity data relevant to Figure 3. (**A-B**) H5 and (**C-D**) H7-binding IgG (A, C) post-prime and (B, D) post-boost serum titers. (**E**) H5N1 and (**F**) H7N9 neutralization capacity (IC_{50}) of post-boost mouse serum. (**G-I**) Post-boost H5-reactive splenic (G) polyfunctional (IFN γ^+ IL-2^+ TNF α^+) $CD4^+$ T cells, (H) polyfunctional (IFN γ^+ IL-2^+ TNF α^+) $CD8^+$ T cells, and (I) IFN γ^+ $CD8^+$ T cells. (**J-L**) Post-boost H7-reactive splenic (J) polyfunctional (IFN γ^+ IL-2^+ TNF α^+) $CD4^+$ T cells, (K) polyfunctional (IFN γ^+ IL-2^+ TNF α^+) $CD8^+$ T cells, and (L) IFN γ^+ $CD8^+$ T cells. For all assays, $n = 6$ animals for vector control (SEAP) group, $n = 8$ for experimental groups. All groups were sex balanced. Two statistical hypotheses were tested within each figure, unless specifically listed, with filled lines showing comparisons to the vector control and dotted lines representing tests between key experimental groups. (A-D) Statistical analyses performed on log-transformed data using one-way ANOVA with Dunnett's (filled lines) or Tukey's (dotted lines) multiple comparisons test. (E-F) Statistical analysis performed on log-transformed data used Kruskal-Wallis test with Dunn's multiple comparisons. (G-J) Statistical analysis represents Kruskal-Wallis test with Dunn's multiple comparisons (filled lines [G-J] and dotted lines [H, I]), one-way ANOVA with Tukey's multiple comparisons (dotted lines [G, J, L]), or Brown-Forsythe and Welch ANOVA with Dunnett's T3 multiple comparisons (dotted lines [K]). Data are presented as (A-F) geometric mean +/- geometric SD. LLOD = lower limit of detection; ns = not significant. * $p < 0.05$, ** $p < 0.01$, *** $p < 0.001$, **** $p < 0.0001$. Source data are provided as a Source Data file.

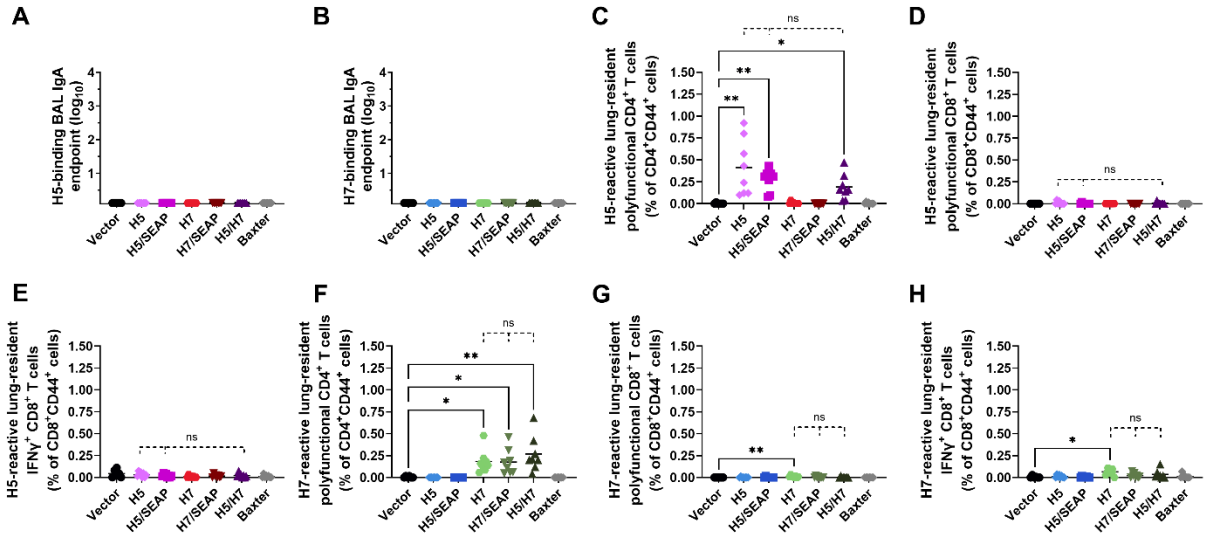

Supplementary Figure 9. Full bivalent intramuscular study mucosal immunogenicity data relevant to Figure 3. Post-boost (**A**) H5 and (**B**) H7-binding IgA antibody titers in BAL samples. (**C-E**) Post-boost H5-reactive lung-resident ($CD69^+$) (C) polyfunctional (IFN γ^+ IL-2^+ TNF α^+) $CD4^+$ T cells, lung-resident ($CD69^+$ $CD103^+$) (D) polyfunctional (IFN γ^+ IL-2^+ TNF α^+) $CD8^+$ T cells, and lung-resident ($CD69^+$ $CD103^+$) (E) IFN γ^+ $CD8^+$ T cells. (**F-H**) Post-boost H7-reactive lung-resident ($CD69^+$) (F) polyfunctional (IFN γ^+ IL-2^+ TNF α^+) $CD4^+$ T cells, lung-resident ($CD69^+$ $CD103^+$) (G) polyfunctional (IFN γ^+ IL-2^+ TNF α^+) $CD8^+$ T cells, and lung-resident ($CD69^+$ $CD103^+$) (H) IFN γ^+ $CD8^+$ T cells. For all assays, $n = 6$ animals for vector control (SEAP) group, $n = 8$ for experimental groups. All groups were sex balanced. Two statistical hypotheses were tested within each figure, unless specifically listed, with filled lines showing comparisons to the vector control) and dotted lines representing tests between key experimental groups. (C-H) Statistical analysis represents Kruskal-Wallis test with Dunn's multiple comparisons (filled lines [C-H] and dotted lines [D, F-H]), one-way ANOVA with Tukey's multiple comparisons (dotted lines [E]), or Brown-Forsythe and Welch ANOVA with Dunnett's T3 multiple comparisons (dotted lines [C]). Data are presented as (A, B) mean +/- SD. ns = not significant. * $p < 0.05$, ** $p < 0.01$. Source data are provided as a Source Data file.

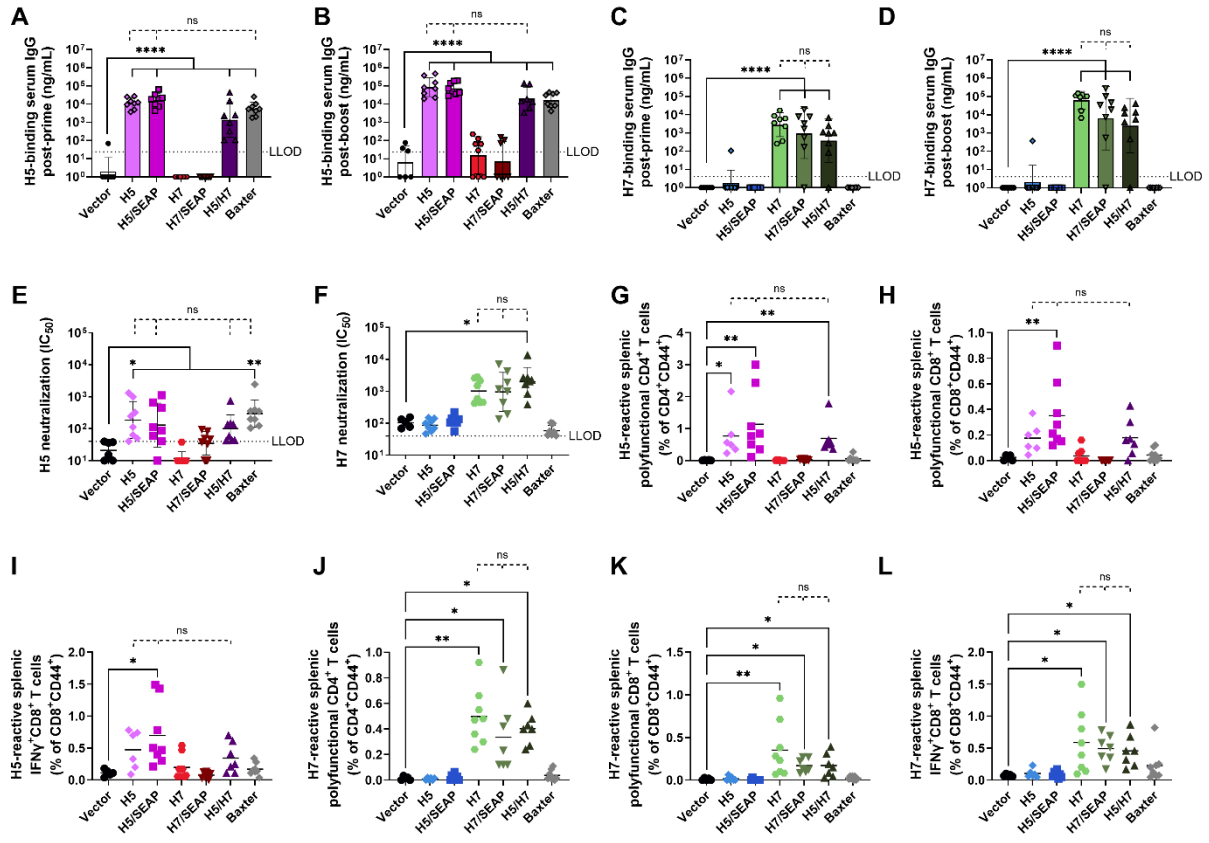

Supplementary Figure 10. Full bivalent intranasal study systemic immunogenicity data relevant to Figure 4. Serum (**A-B**) H5 and (**C-D**) H7-binding IgG titers (A, C) post-prime and (B, D) post-boost. Post-boost serum (**E**) H5 and (**F**) H7 pseudovirus neutralization capacity (IC_{50}). (**G-I**) Post-boost H5-reactive splenic (G) polyfunctional (IFN γ^+ IL-2^+ TNF α^+) $CD4^+$ T cells, (H) polyfunctional (IFN γ^+ IL-2^+ TNF α^+) $CD8^+$T cells, and (I) IFN γ^+ $CD8^+$ T cells. (**J-L**) Post-boost H7-reactive splenic (J) polyfunctional (IFN γ^+ IL-2^+ TNF α^+) $CD4^+$ T cells, (K) polyfunctional (IFN γ^+ IL-2^+ TNF α^+) $CD8^+$ T cells, and (L) IFN γ^+ $CD8^+$ T cells. For all assays, $n = 6$ animals for vector control (SEAP) group, $n = 8$ for experimental groups. All groups were sex balanced. Two statistical hypotheses were tested within each figure, unless specifically listed, with filled lines showing comparisons to the vector control and dotted lines representing tests between key experimental groups. (A-D) Statistical analyses performed on log-transformed data using one-way ANOVA with Dunnett's (filled lines) or Tukey's (dotted lines) multiple comparisons test. (E-F) Statistical analysis performed on log-transformed data used Kruskal-Wallis test with Dunn's multiple comparison test. (G-L) Statistical analysis represents Kruskal-Wallis test with Dunn's multiple comparisons (filled lines [G-L] and dotted lines [G, H]) or one-way ANOVA with Tukey's multiple comparisons (dotted lines [I-L]). Data are presented as (A-F) geometric mean +/- geometric SD. LLOD = lower limit of detection; ns = not significant. * $p < 0.05$, ** $p < 0.01$, *** $p < 0.001$, **** $p < 0.0001$. Source data are provided as a Source Data file.

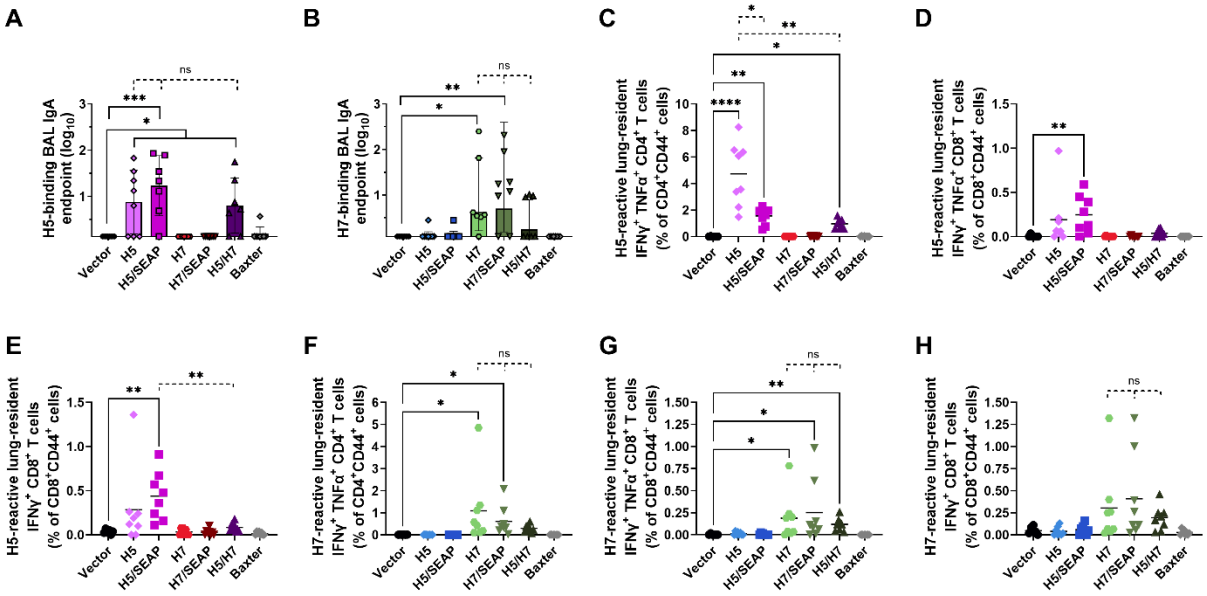

Supplementary Figure 11. Full bivalent intranasal study mucosal immunogenicity data relevant to Figure 4. Post-boost (**A**) H5 and (**B**) H7-binding IgA antibody titers in BAL samples. (**C-E**) Post-boost H5-reactive lung-resident ($CD69^+$) (C) bifunctional ($IFN\gamma^+$ $TNF\alpha^+$) $CD4^+$ T cells, lung-resident ($CD69^+$ $CD103^+$) (D) bifunctional ($IFN\gamma^+$ $TNF\alpha^+$) $CD8^+$ T cells, and lung-resident ($CD69^+$ $CD103^+$) (E) $IFN\gamma^+$ $CD8^+$ T cells. (**F-H**) Post-boost H7-reactive lung-resident ($CD69^+$) (F) bifunctional ($IFN\gamma^+$ $TNF\alpha^+$) $CD4^+$ T cells, lung-resident ($CD69^+$ $CD103^+$) (G) bifunctional ($IFN\gamma^+$ $TNF\alpha^+$) $CD8^+$ T cells, and lung-resident ($CD69^+$ $CD103^+$) (H) $IFN\gamma^+$ $CD8^+$ T cells. For all assays, $n = 6$ animals for vector control (SEAP) group, $n = 8$ for experimental groups. All groups were sex balanced. Two statistical hypotheses were tested within each figure, with filled lines showing comparisons to the vector control and dotted lines representing tests between key experimental groups. (A-B) Statistical analyses performed on log-transformed data using one-way ANOVA with Dunnett's (filled lines) or Tukey's (dotted lines) multiple comparisons test. (C-H) Statistical analysis represents Kruskal-Wallis test with Dunn's multiple comparisons (filled lines [C-H] and dotted lines [D-H]) or Brown-Forsythe and Welch ANOVA with Dunnett's T3 multiple comparisons (dotted lines [C]). Data are presented as (A, B) mean +/- SD. ns = not significant. * $p < 0.05$, ** $p < 0.01$, ***$p < 0.001$, **** $p < 0.0001$. Source data are provided as a Source Data file.

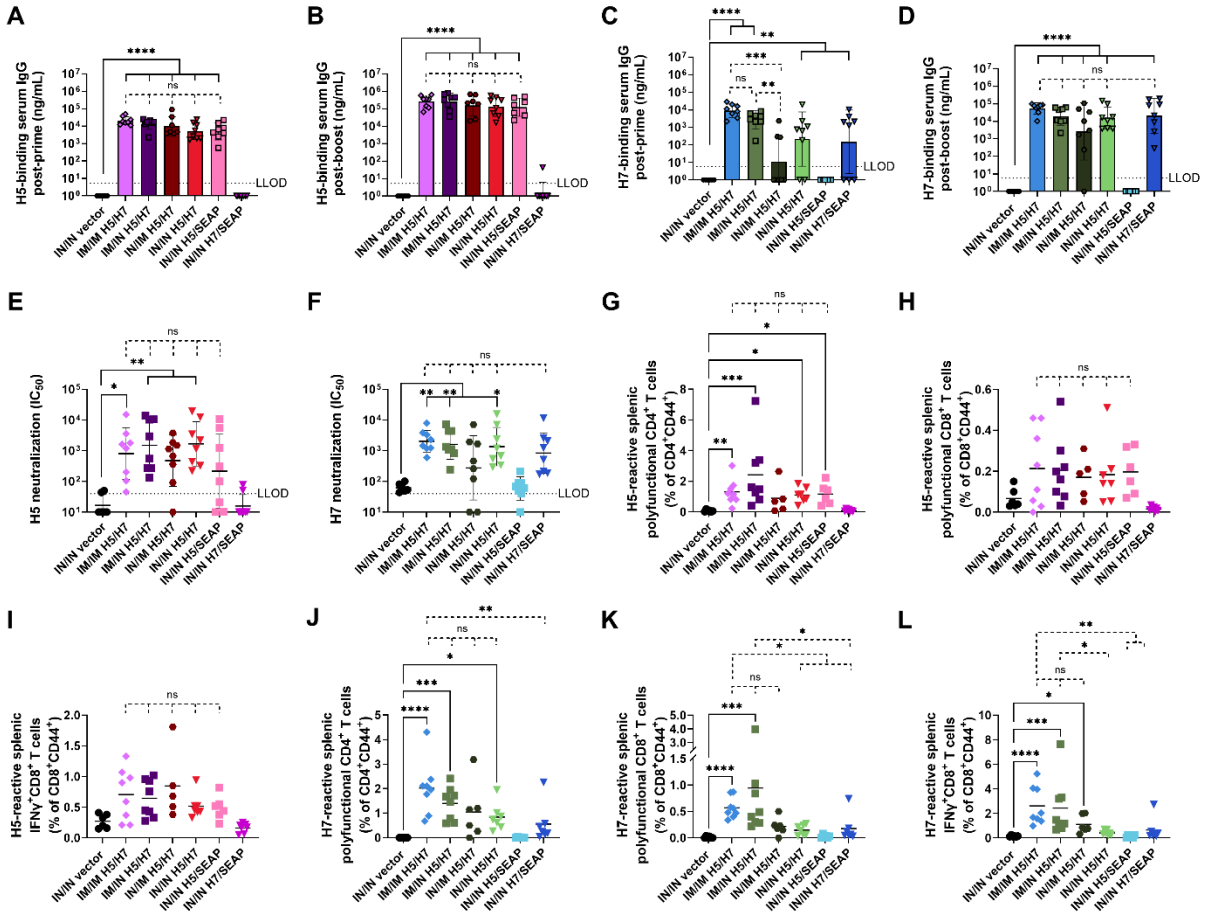

Supplementary Figure 12. Additional systemic immunogenicity data for the routes of bivalent vaccination study presented in Figure 5. (**A-B**) H5 and (**C-D**) H7-binding IgG (A, C) post-prime and (B, D) post-boost serum IgG titers. (**E**) H5N1 and (**F**) H7N9 neutralization capacity (IC_{50}) of post-boost mouse serum. (**G-I**) Post-boost H5-reactive splenic (G) polyfunctional ($IFN\gamma^+$ $IL\text{-}2^+$ $TNF\alpha^+$) $CD4^+$ T cells, (H) polyfunctional ($IFN\gamma^+$ $IL\text{-}2^+$ $TNF\alpha^+$) $CD8^+$ T cells, and (I) $IFN\gamma^+$ $CD8^+$ T cells. (**J-L**) Post-boost H7-reactive splenic (J) polyfunctional ($IFN\gamma^+$ $IL\text{-}2^+$ $TNF\alpha^+$) $CD4^+$ T cells, (K) polyfunctional ($IFN\gamma^+$ $IL\text{-}2^+$ $TNF\alpha^+$) $CD8^+$ T cells, and (L) $IFN\gamma^+$ $CD8^+$ T cells. For all assays, $n = 6$ animals for vector control (SEAP) group, $n = 8$ for experimental groups. All groups were sex balanced. Two statistical hypotheses were tested within each figure, unless specifically listed, with filled lines showing comparisons to the vector control and dotted lines representing tests between key experimental groups. (A-D) Statistical analyses performed on log-transformed data using one-way ANOVA with Dunnett's (filled lines) or Tukey's (dotted lines) multiple comparisons test. (E-F) Statistical analysis performed on log-transformed data used Kruskal-Wallis test with Dunn's multiple comparisons. (G-L) Statistical analysis represents Kruskal-Wallis test with Dunn's multiple comparisons (filled lines [G, H, J-L] and dotted lines [G, J-L]), one-way ANOVA with Tukey's multiple comparisons (dotted lines [H, I]), or Brown-Forsythe and Welch ANOVA with Dunnett's T3 multiple comparisons (filled lines [I]). Data are presented as (A-F) geometric mean +/- geometric SD. LLOD = lower limit of detection; ns = not significant. * $p < 0.05$, ** $p < 0.01$, *** $p < 0.001$, **** $p < 0.0001$. Source data are provided as a Source Data file.

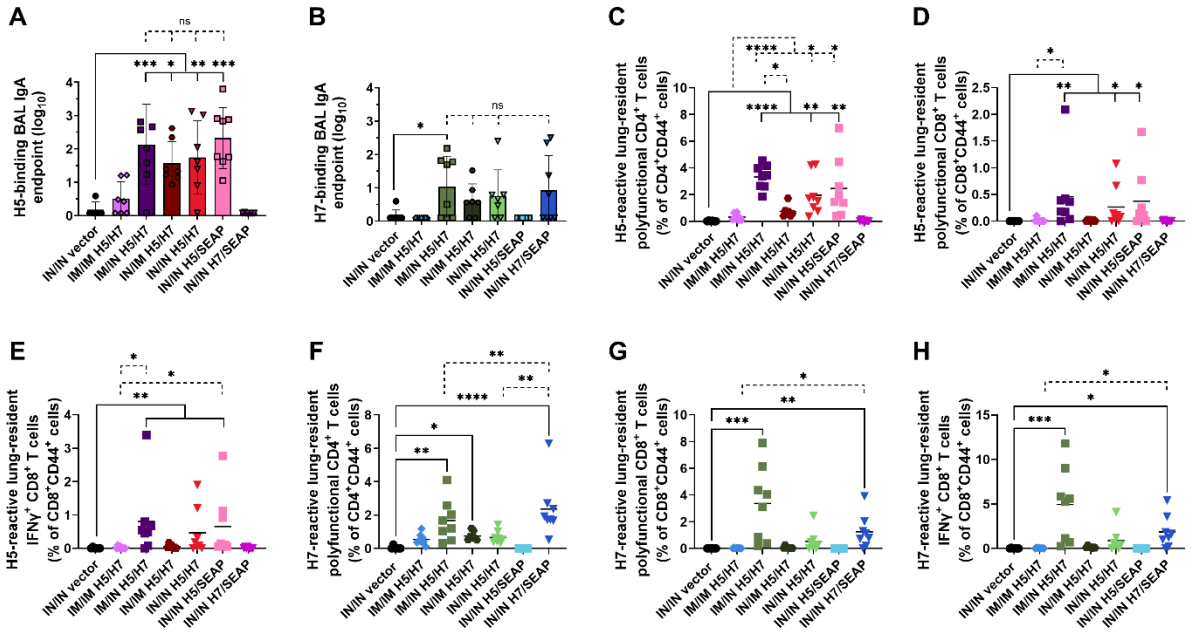

Supplementary Figure 13. Additional mucosal immunogenicity data for the routes of bivalent vaccination study presented in Figure 5. (**A**) H5 and (**B**) H7-binding IgA antibody titers in mouse BAL material post-boost. (**C-E**) Post-boost H5-reactive lung-resident ($CD69^+$) (C) polyfunctional ($IFN\gamma^+$ $IL\text{-}2^+$ $TNF\alpha^+$) $CD4^+$ T cells, lung-resident ($CD69^+$ $CD103^+$) (D) polyfunctional ($IFN\gamma^+$ $IL\text{-}2^+$ $TNF\alpha^+$) $CD8^+$ T cells, and lung-resident ($CD69^+$ $CD103^+$) (E) $IFN\gamma^+$ $CD8^+$ T cells. (**F-H**) Post-boost H7-reactive lung-resident ($CD69^+$) (F) polyfunctional ($IFN\gamma^+$ $IL\text{-}2^+$ $TNF\alpha^+$) $CD4^+$ T cells, lung-resident ($CD69^+$ $CD103^+$) (G) polyfunctional ($IFN\gamma^+$ $IL\text{-}2^+$ $TNF\alpha^+$) $CD8^+$ T cells, and lung-resident ($CD69^+$ $CD103^+$) (H) $IFN\gamma^+$ $CD8^+$ T cells. For all assays, $n = 6$ animals for vector control (SEAP) group, $n = 8$ for experimental groups. All groups were sex balanced. Two statistical hypotheses were tested within each figure, with filled lines showing comparisons to the vector control and dotted lines representing tests between key experimental groups. (A-B) Statistical analyses performed on log-transformed data using one-way ANOVA with Dunnett's (filled lines) or Tukey's (dotted lines) multiple comparisons test. (C-H) Statistical analysis represents Kruskal-Wallis test with Dunn's multiple comparisons (filled lines and dotted lines). Data are presented as (A, B) mean +/- SD. ns = not significant. * $p < 0.05$, ** $p < 0.01$, *** $p < 0.001$, **** $p < 0.0001$. Source data are provided as a Source Data file.

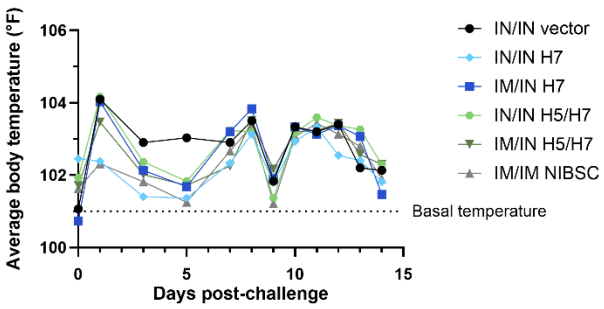

Supplementary Figure 14. Ferret body temperature after H7N9 challenge. *n* = 6 (3 male and 3 female) animals per group. NIBSC = NIBSC Influenza Antigen A/Anhui/1/2013 (H7N9). IN = Intranasal; IM = Intramuscular. Source data are provided as a Source Data file.

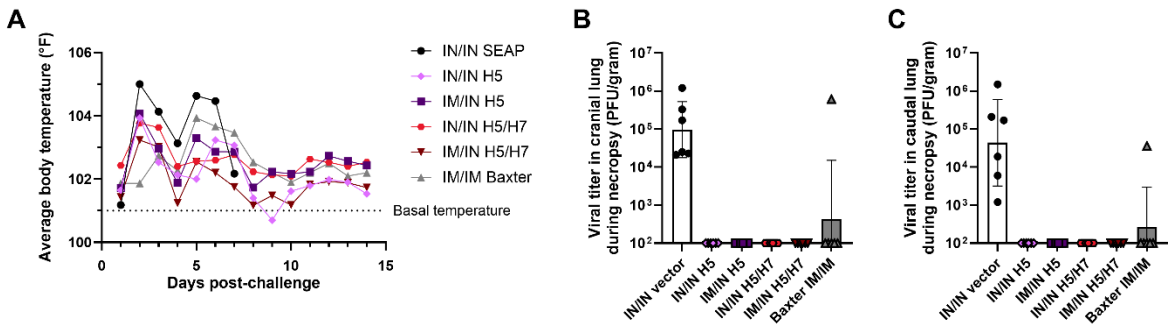

Supplementary Figure 15. Additional metrics for tracking ferret outcomes post-H5N1 challenge. (A) Ferret body temperature. *n* = 6 (3 male and 3 female) animals per group. **(B-C)** Viral titers in lung tissue at necropsy. Data are presented as (B, C) geometric mean +/- geometric SD. IN = Intranasal; IM = Intramuscular. Source data are provided as a Source Data file.

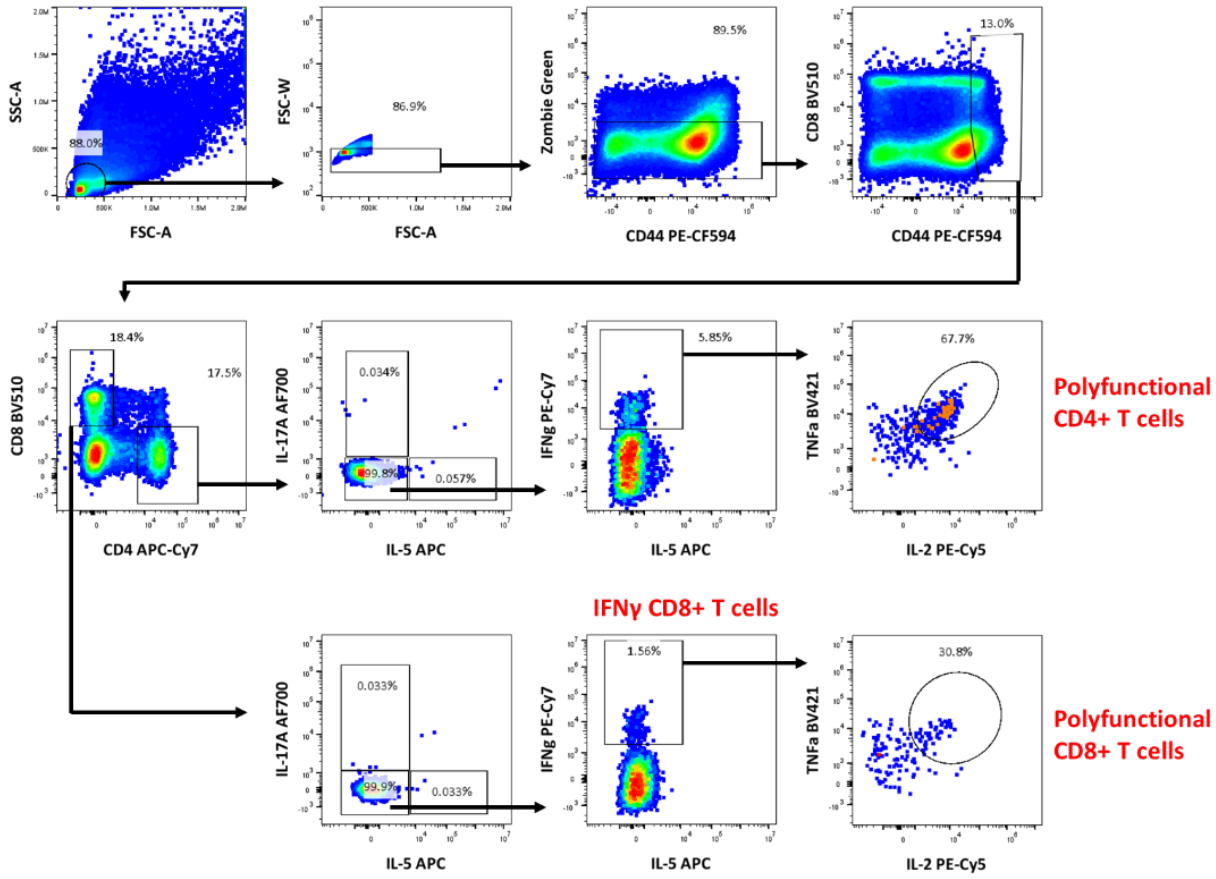

Supplementary Figure 16. Representative splenic T cell ICS flow cytometry gating strategy. Biplots depict the gating strategy used to identify polyfunctional ($TNF\alpha^+$ $IL\text{-}2^+$ $IFN\gamma^+$) $CD4^+$ T cells, polyfunctional $CD8^+$ T cells, and $IFN\gamma^+$ $CD8^+$ T cells isolated from mouse spleens. Data shown are from splenocytes stimulated *in vitro* with an H7 peptide pool following prime/boost IM/IM immunization with the H5/H7 bivalent replicon-NLC vaccine. IM = Intramuscular; NLC = nanostructured lipid carrier.

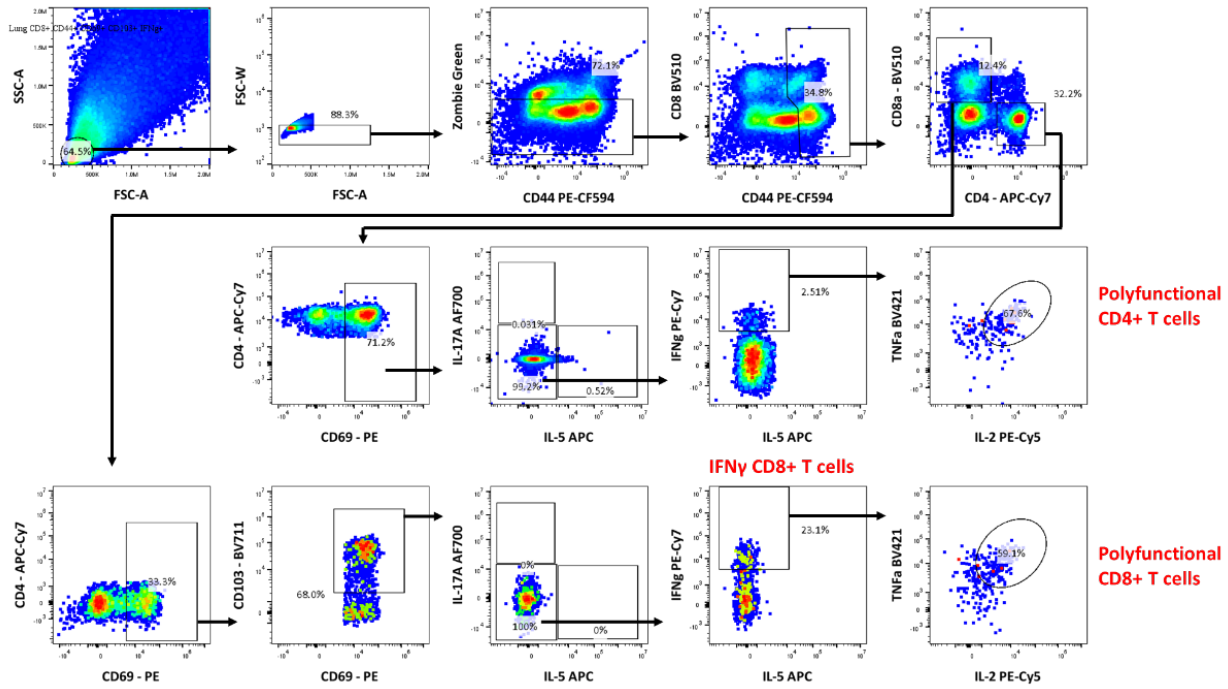

Supplementary Figure 17. Representative lung T cell ICS flow cytometry gating strategy. Biplots depict the gating strategy used to identify polyfunctional ($TNF\alpha^+$ $IL\text{-}2^+$ $IFN\gamma^+$) $CD4^+$ T cells, polyfunctional $CD8^+$ T cells, and $IFN\gamma^+$ $CD8^+$ T cells isolated from mouse lungs. Data shown are from lung lymphocytes stimulated *in vitro* with an H7 peptide pool following prime/boost IM/IN immunization with the H5/H7 bivalent replicon-NLC vaccine. IN = Intranasal; IM = Intramuscular; NLC = nanostructured lipid carrier.